Inorganic Chemistry
Article

Inorg. Chem. **2010**, *49*, 7521–7529 **7521**
DOI: 10.1021/ic1008347

Transition Metal Complexes Supported by a Neutral Tetraamine Ligand Containing *N,N*-dimethylaniline Units

Lei Chu, Kenneth I. Hardcastle, and Cora E. MacBeth*

Department of Chemistry, Emory University, Atlanta, Georgia 30322

Received April 27, 2010

First-row transition metal-halide complexes of tris(2-dimethylaminophenyl)amine, L^{Me}, have been synthesized and characterized. X-ray crystallographic studies on $[Co(L^{Me})Br]BPh_4$, $[Ni(L^{Me})Cl]BPh_4$, $[Fe(L^{Me})Cl]BPh_4$, and $[Cu(L^{Me})Cl]BF_4$ have been performed, and in all cases the ligand produces five-coordinate complexes with distorted trigonal bipyramidal coordination geometries. Where possible, comparisons have been made to the structures of related neutral tripodal ligands. Spectroscopic and magnetic studies of these complexes are also described. The Cu(I)-carbonyl complexes $[Cu(L^{Me})(CO)]PF_6$ and $[Cu(Me_6tren)(CO)]PF_6$ (Me_6tren = tris(*N,N*-dimethylaminoethyl)amine) have also been prepared. Infrared spectroscopic investigations of these carbonyl complexes confirm that L^{Me} is a less electron donating ligand than Me_6tren and indicate that L^{Me} can impart a different coordination number in the solid-state.

Introduction

Research in the area of multidentate ligand design is motivated by the tenet that ancillary ligands play important roles in regulating metal ion reactivity by influencing the geometric, steric, and electronic features of the coordinated metal ions.[1] Within this field, neutral, tripodal, tetraamine ligands have been widely studied.[1−3] They have been utilized extensively in biomimetic copper[4−15] and iron[16−23] chemistry and as supporting scaffolds for copper-mediated atom-transfer radical polymerization (ATRP).[24−31] Some of the most familiar ligands in this class include tris(2-aminoethyl)amine (tren), tris(*N,N*-dimethylaminoethyl)amine (Me_6tren), and tris(2-pyridylmethyl)amine (TMPA), Chart 1.

*To whom correspondence should be addressed. E-mail: cora.macbeth@emory.edu.

(1) Pettinari, C.; Marchetti, F.; Drozdov, A. *Compr. Coord. Chem. II* **2004**, *1*, 211–251.
(2) Blackman, A. G. *Eur. J. Inorg. Chem.* **2008**, *17*, 2633–2647.
(3) Blackman, A. G. *Polyhedron* **2005**, *24*(1), 1–39.
(4) Suzuki, M. *Acc. Chem. Res.* **2007**, *40*(7), 609–617.
(5) Komiyama, K.; Furutachi, H.; Nagatomo, S.; Hashimoto, A.; Hayashi, H.; Fujinami, S.; Suzuki, M.; Kitagawa, T. *Bull. Chem. Soc. Jpn.* **2004**, *77*(1), 59–72.
(6) Hatcher, L. Q.; Karlin, K. D. *Adv. Inorg. Chem.* **2006**, *58*, 131–184.
(7) Dittler-Klingemann, A. M.; Hahn, F. E. *Inorg. Chem.* **1996**, *35*(7), 1996–1999.
(8) Karlin, K. D.; Kim, E. *Chem. Lett.* **2004**, *33*(10), 1226–1231.
(9) Becker, M.; Heinemann, F. W.; Schindler, S. *Chem.—Eur. J.* **1999**, *5*(11), 3124–3129.
(10) Wuertele, C.; Sander, O.; Lutz, V.; Waitz, T.; Tuczek, F.; Schindler, S. *J. Am. Chem. Soc.* **2009**, *131*(22), 7544–7545.
(11) Lee, Y.; Park, G.-Y.; Lucas, H. R.; Vajda, P. L.; Kamaraj, K.; Vance, M. A.; Milligan, A. E.; Woertink, J. S.; Siegler, M. A.; Narducci Sarjeant, A. A.; Zakharov, L. N.; Rheingold, A. L.; Solomon, E. I.; Karlin, K. D. *Inorg. Chem.* **2009**, *48*(23), 11297–11309.
(12) Fry, H. C.; Lucas, H. R.; Narducci Sarjeant, A. A.; Karlin, K. D.; Meyer, G. J. *Inorg. Chem.* **2008**, *47*(1), 241–256.
(13) Wuertele, C.; Gaoutchenova, E.; Harms, K.; Holthausen, M. C.; Sundermeyer, J.; Schindler, S. *Angew. Chem., Int. Ed.* **2006**, *45*(23), 3867–3869.
(14) Hatcher, L. Q.; Karlin, K. D. *J. Biol. Inorg. Chem.* **2004**, *9*(6), 669–683.
(15) Karlin, K. D.; Hayes, J. C.; Juen, S.; Hutchinson, J. P.; Zubieta, J. *Inorg. Chem.* **1982**, *21*(11), 4106–4108.
(16) Britovsek, G. J. P.; England, J.; White, A. J. P. *Inorg. Chem.* **2005**, *44*(22), 8125–8134.
(17) Lim, M. H.; Rohde, J.-U.; Stubna, A.; Bukowski, M. R.; Costas, M.; Ho, R. Y. N.; Munck, E.; Nam, W.; Que, L. Jr. *Proc. Natl. Acad. Sci. U. S. A.* **2003**, *100*(7), 3665–3670.
(18) Jensen, M. P.; Lange, S. J.; Mehn, M. P.; Que, E. L.; Que, L., Jr. *J. Am. Chem. Soc.* **2003**, *125*(8), 2113–2128.
(19) Que, L., Jr.; Dong, Y. *Acc. Chem. Res.* **1996**, *29*(4), 190–196.
(20) Mandon, D.; Machkour, A.; Goetz, S.; Welter, R. *Inorg. Chem.* **2002**, *41*(21), 5364–5372.
(21) Diebold, A.; Hagen, K. S. *Inorg. Chem.* **1998**, *37*(2), 215–223.
(22) Chen, K.; Que, L., Jr. *J. Am. Chem. Soc.* **2001**, *123*(26), 6327–6337.
(23) Costas, M.; Que, L., Jr. *Angew. Chem., Int. Ed.* **2002**, *41*(12), 2179–2181.
(24) Cohen, N. A.; Tillman, E. S.; Thakur, S.; Smith, J. R.; Eckenhoff, W. T.; Pintauer, T. *Macromol. Chem. Phys.* **2009**, *210*(3−4), 263–268.
(25) Baisch, U.; Poli, R. *Polyhedron* **2008**, *27*(9−10), 2175–2185.
(26) Pintauer, T.; Braunecker, W.; Collange, E.; Poli, R.; Matyjaszewski, K. *Macromolecules* **2004**, *37*(8), 2679–2682.
(27) Matyjaszewski, K.; Xia, J. *Chem. Rev.* **2001**, *101*(9), 2921–2990.
(28) Wang, J.-S.; Matyjaszewski, K. *J. Am. Chem. Soc.* **1995**, *117*(20), 5614–5615.
(29) Pintauer, T.; Matyjaszewski, K. *Chem. Soc. Rev.* **2008**, *37*(6), 1087–1097.
(30) Pintauer, T.; Matyjaszewski, K. *Coord. Chem. Rev.* **2005**, *249*(11−12), 1155–1184.
(31) Eckenhoff, W. T.; Pintauer, T. *Catal. Rev. - Sci. Eng.* **2010**, *52*(1), 1–59.

Published on Web 07/21/2010

Chart 1

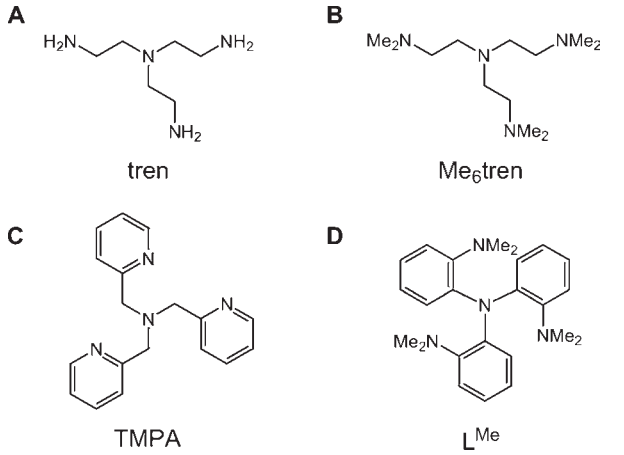

Recent research in the areas of dioxygen activation by Cu(I)[4−6,8,11,13,32−34] and hydrogen peroxide activation by Fe(II)[16,35−37] complexes has demonstrated that the electronic and steric requirements of the tetraamine ligands play a crucial role in regulating the reactivity of these complexes. For example, Karlin and co-workers synthesized a series of electronically varied ligands based on the TMPA scaffold by introducing non-hydrogen substituents into the 4-pyridyl position of the ligand, $TMPA^{R}$.[38] In weakly coordinating solvents they found that the ligands with the greatest electron donating ability (i.e., $TMPA^{OMe}$ and $TMPA^{NMe2}$) increased the thermodynamic stability of the resulting $[(TMPA^{R})Cu^{II}(O_2^{-})]^{+}$ and $[\{(TMPA^{R})Cu\}_2(\mu\text{-}1,2\text{-}O_2^{2-})]^{2+}$ complexes and decreased the dissociation rates of these species. These results were expected because dioxygen binding to Cu(I) centers is a redox process that requires oxidation to Cu(II), which would be favored by more electron-releasing ligand scaffolds. In other work, Britovsek and co-workers investigated the reactivity of hydrogen peroxide with a series of Fe(II) bis(triflate) complexes supported by neutral, tetraamine ligands as alkane oxidation catalysts.[16,37] They found that the solution-state structures of the bis(triflate) complexes and the mechanism of alkane oxidation was dependent on the chelating ligands. These studies demonstrated that ligands containing two or more pyridyl groups favored six-coordinate species and prevented Fenton-type reaction chemistry.[16] Subsequent studies by these researchers using magnetic and spectroscopic studies confirmed that ligand rigidity and, therefore, catalyst stability under oxidizing conditions is a key determinant in the overall catalytic activity of these species.[37]

Our group recently reported the coordination chemistry of Co(II) with tris(2-aminophenyl)amine, $N(o\text{-}PhNH_2)_3$, a tetradentate ligand system that incorporates *o*-phenylenediamine donors into the ligand backbone.[39] We speculated that the incorporation of the *o*-phenylenediamine unit into a tripodal ligand would result in a more rigid, chelating tetraamine framework that could display non-innocent behavior.[40] Further functionalization of tris(2-aminophenyl)amine to form trianionic tris(amidate)amine[39,41−43] and tris(amido)amine ligands[43−46] has since been described, but uncharged ligands based on the $N(o\text{-}PhNH_2)_3$ unit that lack reactive protons have remained unexplored. In an effort to create neutral, tetradentate, tripodal ligand systems that produce metal complexes with more rigid solution and solid-state topologies and possess different electronic properties from their corresponding alkyl amine and pyridyl counterparts, we sought to synthesize and explore the coordination chemistry of $N(o\text{-}PhNMe_2)_3$, L^{Me}. We chose to target the hexamethyl derivative because methyl substituents are relatively small, and we wanted to make a direct comparison with Me_6tren. We anticipated that any differences observed between L^{Me} and Me_6tren could be attributed to the incorporation of the rigid aryl backbone. Here, we describe the synthesis, coordination chemistry, and spectral properties of later, first-row transition metal ions supported by L^{Me}. The M^{II}-halide complexes, $[M^{II}(L^{Me})X]^{+}$, of this ligand have been compared to similar complexes supported by tetradentate ligands that incorporate alkyl units or pyridine rings into the five-membered, chelating rings. The spectroscopic and magnetic properties for the $[M^{II}(L^{Me})X]^{+}$ series of complexes have been measured and used to provide information about the ligand field strength of L^{Me}. Finally, the Cu(I) carbonyl complexes of L^{Me} and Me_6tren ($[Cu(L^{Me})(CO)]^{+}$ and $[Cu(Me_6tren)(CO)]^{+}$) have been synthesized, characterized, and compared with other Cu(I)-carbonyl complexes supported by tetraamine donor ligands. These carbonyl complexes have been used to probe the electron releasing nature of this class of ligands and to highlight differences in their solid-state and solution-state topologies.

Results and Discussion

Syntheses. The neutral tetraamine ligand tris(2-dimethylaminophenyl)amine, $N(o\text{-}PhNMe_2)_3$ (L^{Me}), was synthesized in good yield by reductive methylation[47,48] of the primary amine precursor, $N(o\text{-}PhNH_2)_3$, (Scheme 1). The ligand can be recrystallized from hot methanol to yield analytically pure material. The L^{Me} scaffold was used to synthesize five first-row transition metal complexes, including four cationic species with the general formula $[M(L^{Me})X]^{+}$ (where M = Fe^{II}, Co^{II}, Ni^{II}, or Cu^{II} and X = Cl^{-} or Br^{-}). A general

(32) Schatz, M.; Becker, M.; Thaler, F.; Hampel, F.; Schindler, S.; Jacobson, R. R.; Tyeklar, Z.; Murthy, N. N.; Ghosh, P.; Chen, Q.; Zubieta, J.; Karlin, K. D. *Inorg. Chem.* **2001**, *40*(10), 2312–2322.
(33) Maiti, D.; Fry, H. C.; Woertink, J. S.; Vance, M. A.; Solomon, E. I.; Karlin, K. D. *J. Am. Chem. Soc.* **2007**, *129*(2), 264–265.
(34) Lucas, H. R.; Li, L.; Narducci Sarjeant, A. A.; Vance, M. A.; Solomon, E. I.; Karlin, K. D. *J. Am. Chem. Soc.* **2009**, *131*(9), 3230–3245.
(35) England, J.; Davies, C. R.; Banaru, M.; White, A. J. P.; Britovsek, G. J. P. *Adv. Synth. Catal.* **2008**, *350*(6), 883–897.
(36) England, J.; Britovsek George, J. P.; Rabadia, N.; White Andrew, J. P. *Inorg. Chem.* **2007**, *46*(9), 3752–3767.
(37) England, J.; Gondhia, R.; Bigorra-Lopez, L.; Petersen, A. R.; White, A. J. P.; Britovsek, G. J. P. *Dalton Trans.* **2009**, *27*, 5319–5334.
(38) Zhang, C. X.; Kaderli, S.; Costas, M.; Kim, E.-i.; Neuhold, Y.-M.; Karlin, K. D.; Zuberbuehler, A. D. *Inorg. Chem.* **2003**, *42*(6), 1807–1824.
(39) Jones, M. B.; MacBeth, C. E. *Inorg. Chem.* **2007**, *46*(20), 8117–8119.
(40) Warren, L. F. *Inorg. Chem.* **1977**, *16*(11), 2814–2819.
(41) Jones, M. B.; Newell, B. S.; Hoffert, W. A.; Hardcastle, K. I.; Shores, M. P.; MacBeth, C. E. *Dalton Trans.* **2010**, *39*(2), 401–410.
(42) Jones, M. B.; Hardcastle, K. I.; MacBeth, C. E. *Polyhedron* **2010**, *29*(1), 116–119.
(43) Paraskevopoulou, P.; Ai, L.; Wang, Q.; Pinnapareddy, D.; Acharyya, R.; Dinda, R.; Das, P.; Celenligil-Cetin, R.; Floros, G.; Sanakis, Y.; Choudhury, A.; Rath, N. P.; Stavropoulos, P. *Inorg. Chem.* **2010**, *49*(1), 108–122.
(44) Celenligil-Cetin, R.; Paraskevopoulou, P.; Lalioti, N.; Sanakis, Y.; Staples, R. J.; Rath, N. P.; Stavropoulos, P. *Inorg. Chem.* **2008**, *47*(23), 10998–11009.
(45) Celenligil-Cetin, R.; Paraskevopoulou, P.; Dinda, R.; Lalioti, N.; Sanakis, Y.; Rawashdeh, A. M.; Staples, R. J.; Sinn, E.; Stavropoulos, P. *Eur. J. Inorg. Chem.* **2008**, *5*, 673–677.
(46) Celenligil-Cetin, R.; Paraskevopoulou, P.; Dinda, R.; Staples, R. J.; Sinn, E.; Rath, N. P.; Stavropoulos, P. *Inorg. Chem.* **2008**, *47*(3), 1165–1172.
(47) Borch, R. F.; Hassid, A. I. *J. Org. Chem.* **1972**, *37*(10), 1673–1674.
(48) Lane, C. F. *Synthesis* **1975**, *3*, 135–146.

Scheme 1

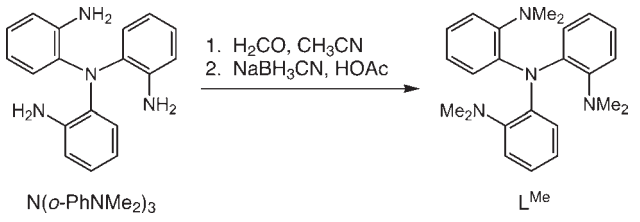

Scheme 2

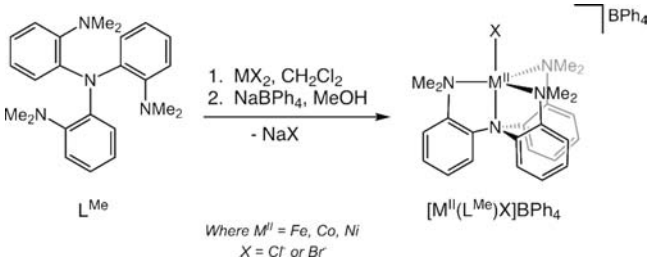

synthetic approach for the preparation of the Fe^{II}, Co^{II}, and Ni^{II} complexes is outlined in Scheme 2.

In a standard metalation procedure, the ligand and an anhydrous metal dihalide salt were stirred together in dichloromethane. In situ counteranion metathesis was then performed by treating the reaction mixture with 1 equiv of sodium tetraphenylborate as a methanol solution. This procedure provides $[Fe(L^{Me})Cl]BPh_4$, $[Co(L^{Me})Br]BPh_4$, and $[Ni(L^{Me})Cl]BPh_4$ in good yields (60−90%). The copper analogue, $[Cu(L^{Me})Cl]BF_4$, was synthesized in a similar manner, except $AgBF_4$ was used in place of $NaBPh_4$. In addition to metallating the ligand with M^{II} ions, we were also interested in exploring its coordination chemistry with Cu(I), given the utility of neutral tetraamine ligands in Cu(I)-dioxygen chemistry. The Cu(I) complex of L^{Me}, $[Cu(L^{Me})]^+$, was synthesized by reacting $[Cu(CH_3CN)_4]PF_6$ directly with L^{Me} in acetonitrile.

X-ray Crystallographic Studies. Attempts to isolate X-ray quality crystals of L^{Me} were unsuccessful. The monoprotonated ligand salt, $[HL^{Me}]PF_6$, however, was readily recrystallized from a mixture of tetrahydrofuran and diethyl ether. The molecular structure of the cationic portion of this species, $[HL^{Me}]^+$, is shown in Figure 1. The acidic proton (H1) was located in the difference map and refined isotropically. The molecular structure of the cation shows H1 residing on one of the *N,N*-dimethylaniline donors (N3). The acidic proton is also interacting with two additional tertiary amine donors (N1 and N2) through hydrogen bonding interactions, as evidenced by the close N3···N2 and N3···N1 through-space distances of 2.932(3) and 2.797(3) Å, respectively. The pyramidalization of the apical nitrogen atom, N1, is approximately halfway between trigonal planar and tetrahedral as the sum of the C_{phenyl}−N1−$C_{phenyl'}$ bond angles ($\sum_{C-N1-C}°$) is 346.3°. This type of pyramidalization is similar to what is observed in the solid-state structure of tris(2-hydroxyphenyl)amine, N(*o*-$C_6H_4OH)_3$.[49]

The Fe(II) complex, $[Fe(L^{Me})Cl]BPh_4$, was crystallized as pale yellow needles by diffusing diethyl ether into an acetonitrile solution of the complex. The complex crystallizes in the *Pc* space group. The molecular structure of $[Fe(L^{Me})Cl]^+$, as determined by X-ray diffraction, is shown in Figure 2A with selected bond lengths and angles listed in Table 1. The equatorial plane about the iron is composed of the three, *N,N*-dimethylaniline ($ArNMe_2$) donor groups. The axial positions are occupied by a chloride ion and the apical tris(aryl)amine (Ar_3N) donor of the ligand backbone. The bond lengths and angles found in $[Fe(L^{Me})Cl]^+$ are similar to the bond lengths and angles observed in $[Fe(Me_6tren)Cl]^+$ (Figure 2B), a closely related iron complex derived from the tris(*N,N*-dimethylaminoethyl)amine (Me_6tren) scaffold. For example, the average Fe1−$N_{equatorial}$ bond length of 2.182(4) Å displayed by $[Fe(L^{Me})Cl]^+$ is slightly longer than the

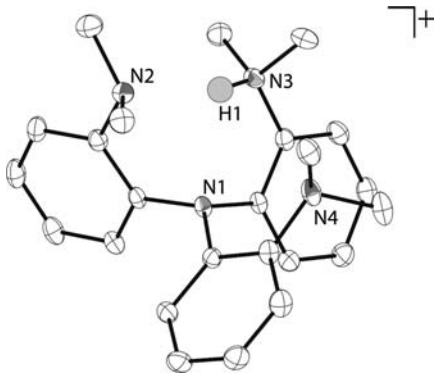

Figure 1. Thermal ellipsoid diagram of $[HL^{Me}]^+$. All of the hydrogen atoms except the acidic proton and the PF_6^- anion and have been removed for clarity.

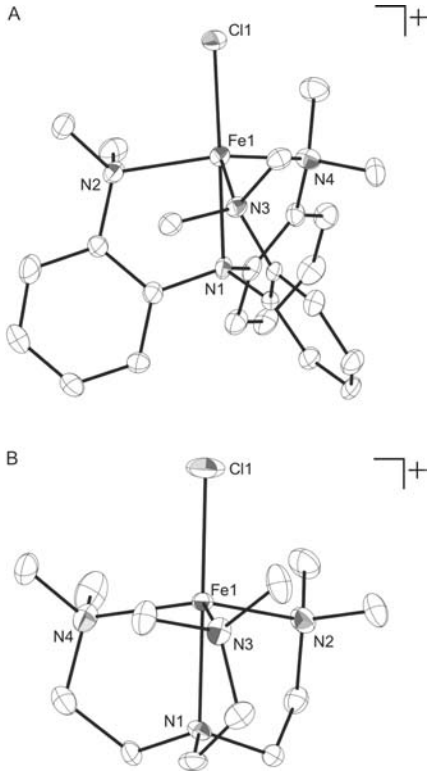

Figure 2. Molecular structure of $[Fe(L^{Me})Cl]BPh_4$ (A) and $[Fe(Me_6tren)Cl]BPh_4$ (B) drawn at 35% probability. Anions and hydrogen atoms have been removed for clarity.

(49) Kelly, B. V.; Tanski, J. M.; Anzovino, M. B.; Parkin, G. *J. Chem. Crystallogr.* **2005**, *35*(12), 969–981.

Table 1. Selected Bond Lengths (Å) and Angles (deg) for $[Fe(L^{Me})Cl]BPh_4$ and $[Fe(Me_6tren)Cl]BPh_4$

	$[Fe(L^{Me})Cl]^+$	$[Fe(Me_6tren)Cl]^+$
Fe1−Cl1	2.287(2)	2.3149(16)
Fe1−N1	2.241(4)	2.234(4)
Fe1−N2	2.179(4)	2.214(4)
Fe1−N3	2.177(4)	2.185(4)
Fe1−N4	2.190(4)	2.202(5)
N1−Fe−Cl1	177.15(11)	178.39(12)
N2−Fe−Cl1	99.76(12)	99.10(12)
N3−Fe−Cl1	104.43(10)	100.59(12)
N4−Fe−Cl1	101.76(13)	99.58(13)
N1−Fe−N2	78.60(15)	80.10(15)
N1−Fe−N3	78.37(13)	81.02(15)
N1−Fe−N4	77.31(15)	79.65(16)
N2−Fe−N3	110.49(15)	116.58(16)
N3−Fe−N4	115.23(14)	116.33(16)
N2−Fe−N4	121.72(15)	118.67(16)

average $Fe1-N_{equatorial}$ bond length of 2.140(4) Å observed in the molecular structure of $[Fe(Me_6tren)Cl]^+$. The axial Fe1−Cl bond length of 2.287(2) Å observed in $[Fe(L^{Me})Cl]^+$ is slightly shorter than the Fe1−Cl bond length of 2.3149(16) Å displayed by $[Fe(Me_6tren)Cl]^+$, while the axial Fe1−N1 bond lengths displayed by both complexes are very similar. The Fe(II) center in $[Fe(L^{Me})Cl]^+$ is positioned 0.45 Å above the equatorial plane while the Fe(II) center in $[Fe(Me_6tren)Cl]^+$ sits 0.37 Å above the equatorial plane. The differences between the two structures can be quantified by calculating the overall five-coordinate structural parameter, τ_5, displayed by the complexes (where $\tau_5 = 1.0$ in an idealized trigonal bipyramidal environment and $\tau_5 = 0.0$ in an idealized square pyramidal coordination geometry).[50] The Fe(II) center in $[Fe(L^{Me})Cl]^+$ lies in a distorted trigonal bipyramidal coordination geometry ($\tau_5 = 0.92$), whereas, the Fe(II) center in $[Fe(Me_6tren)Cl]^+$ is held in an idealized trigonal bipyramidal coordination geometry ($\tau_5 = 1.0$).

The structures of $[Co(L^{Me})Br]BPh_4$, $[Ni(L^{Me})Cl]BPh_4$, and $[Cu(L^{Me})Cl]BF_4$ were also determined by X-ray diffraction studies. The results of these studies are shown in Figure 3, and the metrical parameters for the three complexes are listed in Table 2. For $[Co(L^{Me})Br]BPh_4$, Figure 1A, purple crystals were grown by slowly diffusing ether into a concentrated acetonitrile solution of the complex. The cobalt ion is situated in an idealized trigonal bipyramidal coordination environment ($\tau_5 = 1.0$). The bond lengths between the cobalt ion and the donor atoms are very similar to the cobalt bond lengths displayed by the structurally similar $[Co(Me_6tren)Br]Br$ complex ($\tau_5 = 1.0$).[25,51] For example, the Co1−Br and the average $Co1-N_{equatorial}$ bond lengths of 2.4167(4) Å and 2.1306(19) Å, respectively, in $[Co(L^{Me})Br]^+$ are only slightly shorter than the corresponding bond lengths observed for $[Co(Me_6tren)Br]Br$ (2.4471(7) Å and 2.137(2) Å, respectively). The axial Co1−N1 bond length (2.2280(18) Å) in $[Co(L^{Me})Br]^+$ is somewhat elongated (~ 0.013 Å) compared to the corresponding Co1−N1 bond in $[Co(Me_6tren)Br]Br$. The cobalt center in $[Co(L^{Me})Br]^+$ is distorted 0.41 Å above the equatorial plane formed by the three equatorial amine nitrogen donors toward the bromide ligand.

The nickel complex, $[Ni(L^{Me})Cl]BPh_4$, was crystallized as green needles by the slow diffusion of diethyl ether into a concentrated acetonitrile solution. The molecular structure of $[Ni(L^{Me})Cl]^+$ is shown in Figure 3B, and pertinent bond lengths and angles are listed in Table 2. The nickel center in $[Ni(L^{Me})Cl]^+$ sits in a distorted trigonal bipyramidal coordination geometry ($\tau_5 = 0.86$). The average $Ni1-N_{equatorial}$ (2.110(3) Å) and Ni1−Cl (2.267(1) Å) bond lengths displayed by $[Ni(L^{Me})Cl]^+$, are slightly shorter (ca. 0.02−0.03 Å) than the corresponding bond lengths displayed by the Ni(II) center in the corresponding $[Ni(Me_6tren)Cl]^+$ complexes.[52,53] The Ni(II) center in $[Ni(L^{Me})Cl]^+$ is distorted 0.29 Å out of the equatorial plane toward the halide ligand.

The $[Cu(L^{Me})Cl]BF_4$ was crystallized as light yellow-green blocks from an acetonitrile/diethyl ether solution. The copper(II) ion lies in a slightly distorted trigonal bipyramidal coordination environment ($\tau_5 = 0.97$) and is distorted 0.26 Å out of the equatorial plane. The bond lengths and angles are close to those observed in the related $[Cu(Me_6tren)Cl]^+$ species ($\tau_5 = 1.0$).[9,25] For instance, the average $Cu1-N_{equatorial}$ bond length displayed by $[Cu(L^{Me})Cl]^+$ is 2.144(3) Å compared to 2.186(2) Å for $[Cu(Me_6tren)Cl]^+$.

The preceding X-ray diffraction studies demonstrate that the L^{Me} ligand can be used to stabilize five-coordinate metal complexes with trigonal bipyramidal coordination geometries, and that these complexes have solid-state molecular structures similar to those observed in metal complexes supported by the closely related Me_6tren ligand. Like Me_6tren, L^{Me} appears to have enough steric bulk to prevent the formation of octahedral metal complexes.[52] An important difference between the two scaffolds, however, is that the L^{Me} ligand scaffold gives rise to Fe^{II}, Ni^{II}, and Cu^{II} complexes that display more constrained $N_{equatorial}-M^{II}-N1$ bond angles compared to those observed in the corresponding $[M^{II}(Me_6tren)X]^+$ series of complexes. For each pair of complexes described above, the average $N_{equatorial}-M^{II}-N1$ bond angle in the $[M(L^{Me})X]^+$ complex was about 2° smaller than the corresponding angle in the $[M^{II}(Me_6tren)X]^+$ species. We attribute the smaller $N_{equatorial}-M^{II}-N1$ bond angles (or bite angle) observed in the $[M(L^{Me})X]^+$ series to the slightly more constrained backbone afforded by the L^{Me} ligand framework

Spectroscopic and Magnetic Properties of $[M^{II}(L^{Me})X]^+$ Complexes. All complexes in this study were characterized by infrared, UV−visible, and ^1H NMR spectroscopies. The infrared spectrum of the free ligand exhibits a medium intensity C−N stretching band at 1314 cm^{-1} that shifts to lower frequencies (1300−1255 cm^{-1}) upon metal ion coordination. The $[Fe(L^{Me})Cl]BPh_4$ complex is colorless in solution and gives rise to a paramagnetically broadened ^1H NMR spectrum and a solution magnetic moment of 5.02 μ_B (CD_3CN, 298 K) that is consistent with a high-spin, $S = 2$ ground state. The $[Co(L^{Me})Br]BPh_4$ species is violet in solution and exhibits three absorption bands in its UV−visible absorption spectrum and a magnetic moment of 4.68 μ_B (CD_3CN, 298 K). These data are consistent with

(50) Addison, A. W.; Rao, T. N.; Reedijk, J.; Van Rijn, J.; Verschoor, G. C. *J. Chem. Soc., Dalton Trans.* **1984**, *7*, 1349–1356.
(51) Di Vaira, M.; Orioli, P. *Inorg. Chem.* **1967**, *6*(5), 955–957.
(52) Ciampolini, M.; Nardi, N. *Inorg. Chem.* **1966**, *5*(1), 41–44.
(53) Colpas, G. J.; Kumar, M.; Day, R. O.; Maroney, M. J. *Inorg. Chem.* **1990**, *29*(23), 4779–4788.

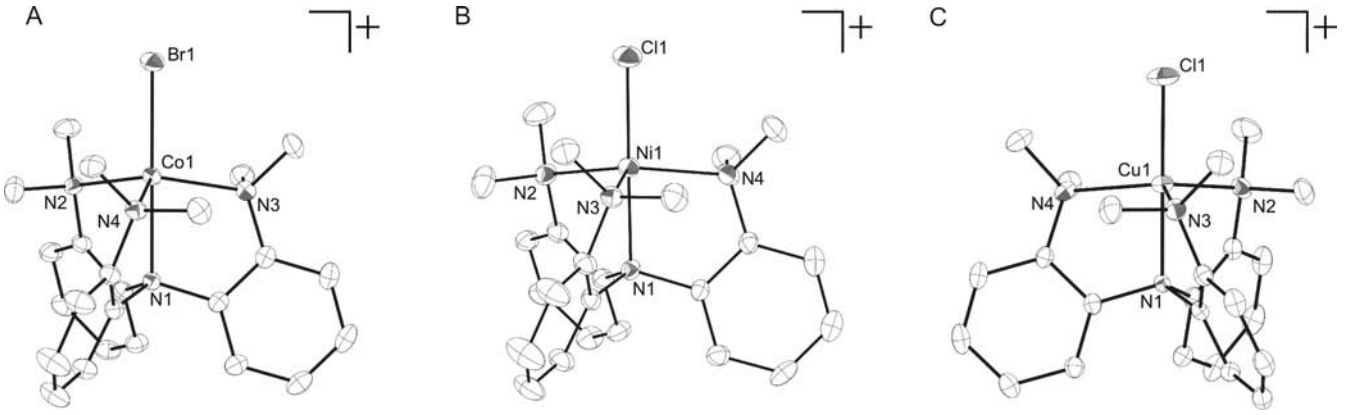

Figure 3. Molecular structures of $[Co(L^{Me})Br]BPh_4$ (A), $[Ni(L^{Me})Cl]BPh_4$ (B), and $[Cu(L^{Me})Cl]BF_4$ (C) drawn at 35% probability. Hydrogen atoms and counteranions have been removed for clarity.

Table 2. Selected Bond Lengths (Å) and Angles (deg) for $[Co(L^{Me})Br]BPh_4$, $[Ni(L^{Me})Cl]BPh_4$, and $[Cu(L^{Me})Cl]BF_4$

	$[Co(L^{Me})Br]^+$	$[Ni(L^{Me})Cl]^+$	$[Cu(L^{Me})Cl]^+$
M1−X1	2.4167(4)	2.2667(13)	2.2121(8)
M1−N1	2.2280(18)	2.114(3)	2.0512(18)
M1−N2	2.1348(19)	2.135(3)	2.131(3)
M1−N3	2.1339(19)	2.080(3)	2.140(3)
M1−N4	2.123(2)	2.114(3)	2.160(3)
N1−M1−X1	178.22(5)	177.26(10)	179.45(11)
N2−M1−X1	100.07(5)	97.56(10)	96.88(7)
N3−M1−X1	100.63(5)	100.05(10)	96.45(8)
N4−M1−X1	102.54(5)	96.62(10)	97.45(8)
N1−M1−N2	78.90(7)	81.32(13)	83.10(9)
N1−M1−N3	78.67(7)	82.69(13)	83.10(10)
N1−M1−N4	79.24(7)	82.10(13)	83.05(11)
N2−M1−N3	117.97(8)	115.33(14)	121.48(10)
N3−M1−N4	115.53(8)	113.09(14)	118.34(10)
N2−M1−N4	115.71(7)	125.81(14)	115.89(10)

an $S = 3/2$ ground state. The green $[Ni(L^{Me})Br]BPh_4$ complex is high spin with a $S = 1$ ground state, ($\mu_{eff} = 3.47\ \mu_B$, (CD_3CN, 298 K)). The magnetic and electronic absorption data for $[Fe(L^{Me})Cl]BPh_4$, $[Co(L^{Me})Br]BPh_4$, and $[Ni(L^{Me})Cl]BPh_4$ suggest that the trigonal bipyramidal geometry observed in their solid-state structures is being maintained in solution.

The electronic absorption spectrum of $[Cu(L^{Me})Cl]BF_4$ exhibits two d-d absorption bands at 782 and 1033 nm with molar extinction coefficients of 146 and 306 $M^{-1}\ cm^{-1}$, respectively. This pattern of one low-energy absorbance accompanied by a higher energy, lower intensity shoulder indicates that a trigonal bipyramidal Cu^{II} coordination geometry is being maintained in solution.[15,32,54] Since $[Cu(L^{Me})Cl]^+$, $[Cu(Me_6tren)Cl]^+$,[9,25] and the closely related $[Cu(TMPA)Cl]^+$[15,32] all display nearly perfect trigonal bipyramidal coordination environments (i.e., solid-state τ_5 values of 0.97, 1.0, and 1.0, respectively) and solution-state electronic absorption spectra consistent with this geometry being maintained in solution, it is possible to compare the absorption maxima for these complexes to determine the relative ligand field strengths for this series of ligands.[5] In Table 3, the d-d transitions for this series of complexes are listed and suggest that Me_6tren, which gives rise to the most blue-shifted spectrum, is the strongest

Table 3. Spectral Data for $[Cu(Me_6tren)Cl]^+$, $[Cu(TMPA)Cl]^+$, and $[Cu(L^{Me})Cl]^+$ in CH_3CN

	λ_{max}/nm (ε/$M^{-1}\ cm^{-1}$)
$[Cu(Me_6tren)Cl]^+$	740 (187), 932 (440)[a]
$[Cu(TMPA)Cl]^+$	632[sh] (90), 962 (210)[b]
$[Cu(L^{Me})Cl]^+$	782 (146), 1033 (306)[c]

[a] Ref 5. [b] Ref 15. [c] This work.

field ligand (Me_6tren (932 nm) > TMPA (955 nm) > L^{Me} (1033 nm)).

To investigate the electron-donating nature of chelating ligands, it can be instructive to compare the carbon monoxide stretching frequencies ($\tilde{\nu}_{CO}$) for the corresponding Cu(I)-carbonyl complexes.[11,12,34,38,55] Karlin and co-workers have also used the infrared spectra of Cu(I)-carbonyl complexes to provide information about solution-state coordination geometries and equilibria.[12,34,56] For example, all three pyridine donors are coordinated in the solid-state molecular structure of $[Cu(TMPA)CO]^+$,[12] and this five-coordinate complex gives rise to a single $\tilde{\nu}_{CO}$ at 2077 cm^{-1} (nujol). In solution, however, the carbonyl stretching frequency shifts to 2090 cm^{-1} in THF and 2092 cm^{-1} in CH_3CN. The shift to higher frequency upon dissolution is attributed to a change in coordination number of the Cu(I) center. They have suggested that an equilibrium exists between the five-coordinate species observed in the solid-state and a four-coordinate species in which one of the ligand arms is dissociated.[11,12] The Cu(I) center in the four-coordinate complex would be less electron-rich and would weaken the carbon monoxide bond to a lesser extent resulting in a larger $\tilde{\nu}_{CO}$ value.

To understand both the electron donating ability of L^{Me} and its solution-state behavior, we set out to synthesize a Cu(I)-carbonyl complex of this ligand. The desired complex, $[Cu(L^{Me})(CO)]^+$, was prepared by bubbling excess carbon monoxide through an acetone solution of $[Cu(L^{Me})]PF_6$. X-ray quality crystals of $[Cu(L^{Me})(CO)]^+$ were obtained by layering a THF solution of the complex with diethyl ether. The molecular structure of $[Cu(L^{Me})(CO)]PF_6$ is shown in Figure 4. The Cu(I) center

(54) Wei, N.; Murthy, N. N.; Karlin, K. D. *Inorg. Chem.* **1994**, *33*(26), 6093–6100.

(55) Laitar, D. S.; Mathison, C. J. N.; Davis, W. M.; Sadighi, J. P. *Inorg. Chem.* **2003**, *42*(23), 7354–7356.

(56) Kretzer, R. M.; Ghiladi, R. A.; Lebeau, E. L.; Liang, H.-C.; Karlin, K. D. *Inorg. Chem.* **2003**, *42*(9), 3016–3025.

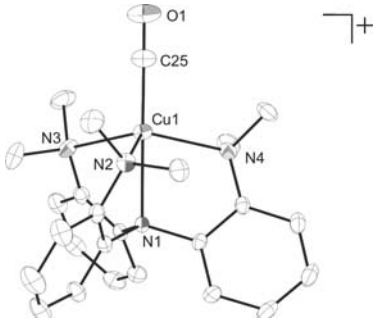

Figure 4. Molecular structure of $[Cu(L^{Me})(CO)]PF_6$ drawn at 35% probability. The anion (PF_6^-) and carbon hydrogen atoms have been removed for clarity. Selected bond lengths (Å) and angles (deg): Cu1−N1 2.347(2), Cu1−N2 2.161(2), Cu1−N3 2.304(2), Cu1−N4 2.245(2), Cu1−C25 1.838(3), C25−O1 1.124(4).

Table 4. Infrared Stretching Frequencies for Cu(I)-Carbonyl Complexes

	ν_{CO} (cm^{-1}) nujol	ν_{CO} (cm^{-1}) THF
$[Cu(Me_6tren)CO]PF_6$	2098	2078
$[Cu(TMPA)CO]PF_6$[a]	2077	2090
$[Cu(L^{Me})CO]PF_6$	2088	2094

[a] Ref 12.

displays a distorted trigonal bipyramidal coordination with an average $Cu-N_{equatorial}$ bond length of 2.24 Å and a Cu−N1 bond length of 2.347(2) Å. The relatively long Cu(I)—N bond lengths[57] in this structure reflect the relatively weak bonding interactions between the Cu(I) center and the L^{Me} ligand. For completeness, the Cu(I)-carbonyl complex of the Me_6tren ligand scaffold has also been prepared and its infrared spectroscopy analyzed. Unfortunately, this complex has yet to be isolated in a crystalline form suitable for X-ray diffraction studies.

The $\tilde{\nu}_{CO}$ values for $[Cu(Me_6tren)CO]^+$, $[Cu(TMPA)CO]^+$, and $[Cu(L^{Me})CO]^+$ are shown in Table 4. The $[Cu(TMPA)CO]^+$ and $[Cu(L^{Me})CO]^+$ complexes show similar trends. Both $[Cu(TMPA)CO]^+$ and $[Cu(L^{Me})CO]^+$ exhibit their lowest $\tilde{\nu}_{CO}$ values (2077 cm^{-1} and 2088 cm^{-1}) in nujol where both complexes are five-coordinate.[11,12,38] When $[Cu(TMPA)CO]^+$ and $[Cu(L^{Me})CO]^+$ are dissolved in THF their $\tilde{\nu}_{CO}$ values shift to slightly higher frequencies (2090 cm^{-1} and 2094 cm^{-1}, respectively) consistent with the presence of four-coordinate species in solution.

The $\tilde{\nu}_{CO}$ values for $[Cu(Me_6tren)CO]^+$ in a nujol mull and in THF (Table 4) have also been recorded. The trends observed for this complex are different. Specifically, $[Cu(Me_6tren)CO]^+$ exhibits its highest $\tilde{\nu}_{CO}$ value in nujol. On the basis of the carbon monoxide stretching frequencies reported for other four-coordinate Cu(I)-carbonyl complexes supported by three uncharged nitrogen donor ligands,[12,58−60] we postulate that in the solid-state, $[Cu(Me_6tren)CO]^+$ exists exclusively as a four-coordinate complex with the Me_6tren ligand coordinating in a

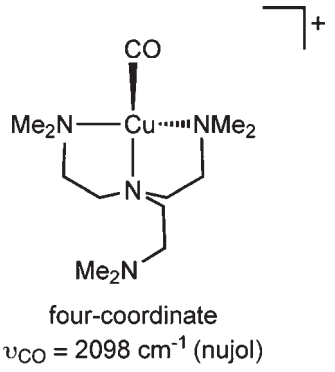

Figure 5. Four-coordinate, κ^3 isomer of $[Cu(Me_6tren)CO]^+$.

κ^3-fashion (Figure 5). The κ^3-coordination mode of Me_6-tren has been observed before in the solid-state molecular structure of a square-planar palladium complex.[61] In THF solutions, the $\tilde{\nu}_{CO}$ for $[Cu(Me_6tren)CO]^+$ shifts to lower frequencies suggesting the possible existence of an equilibrium between the four- and five-coordinate species. Low temperature ^1H NMR experiments were attempted to determine the identity of the five-coordinate species. Specifically, we tried to determine if the five-coordinate species contains the Me_6tren ligand coordinated in a κ^4-coordination mode or if the fifth coordination site is occupied by a coordinating solvent molecule. Unfortunately, these experiements were not conclusive and complicated by the limited solubility of $[Cu(Me_6tren)CO]^+$ in cold d_8-THF. We do, however, note that the $\tilde{\nu}_{CO}$ of $[Cu(Me_6tren)CO]^+$ in solution is sensitive to the nature of the solvent (e.g., $\tilde{\nu}_{CO}$ = 2078 cm^{-1} in THF and $\tilde{\nu}_{CO}$ = 2085 cm^{-1} in CH_3CN) suggesting that a coordinating solvent molecule may be present in the five-coordinate species. The carbonyl stretching frequencies for $[Cu(TMPA)Cl]^+$ and $[Cu(L^{Me})CO]^+$ are consistent with TMPA being more electron donating than L^{Me}. The overall electron donating ability of this series (Me_6tren > TMPA > L^{Me}) should be consistent with the pK_a values of the conjugate acids of the ligand donor groups (i.e., [*N,N*-dimethylethylaminium]$^+$ (9.83 ± 0.28); [2-methylpyridinium]$^+$ (5.95 ± 0.28); and [*N,N*-dimethylbenyzlaminium]$^+$ (5.1 ± 0.28)).[62]

Conclusions

A tetradentate, tetraamine ligand system, L^{Me}, that incorporates *N,N*-dimethylaniline donor groups into a tripodal framework has been synthesized by the reductive amination of $N(o\text{-}PhNH_2)_3$. A series of M^{II}-halide complexes, $[M^{II}(L^{Me})X]^+$, have been synthesized, and their solution-state and solid-state structures evaluated. The rigid aryl backbone of L^{Me} gives rise to five-coordinate, distorted trigonal bipyramidal complexes that exhibit smaller chelate bite angles than those observed in five-coordinate M^{II}-halide complexes supported by its alkyl congener, Me_6tren. Electronic absorption and infrared spectroscopy studies confirm that L^{Me} is a weaker field and less electron-donating ligand than both TMPA and Me_6tren. Comparative infrared spectroscopy studies on the

(57) Orpen, A. G.; Brammer, L.; Allen, F. H.; Kennard, O.; Watson, D. G.; Taylor, R. *J. Chem. Soc., Dalton Trans.* **1989**, *12*, S1–S83.
(58) Kimura, E.; Koike, T.; Kodama, M.; Meyerstein, D. *Inorg. Chem.* **1989**, *28*(15), 2998–3001.
(59) Achternbosch, M.; Apfel, J.; Fuchs, R.; Kluefers, P.; Selle, A. *Z. Anorg. Allg. Chem.* **1996**, *622*(8), 1365–1373.
(60) Kujime, M.; Kurahashi, T.; Tomura, M.; Fujii, H. *Inorg. Chem.* **2006**, *46*(2), 541–551.
(61) Ferguson, G.; Parvez, M. *Acta Crystallogr., Sect. B: Struct. Crystallogr. Cryst. Chem.* **1979**, *B35*(9), 2207–2210.
(62) *Scifinder*, Web version; Chemical Abstracts Service: Columbus, Ohio, 2010. Calculated using Advanced Chemistry Development (ACD/Labs) Software version V8.14 (1994−2010) RN: 121-69-7, 109-06-8, and 598-56-1.

Cu(I)-carbonyl complexes $[Cu(Me_6tren)CO]^+$ and $[Cu(L^{Me})CO]^+$ suggest these ligands can adopt different coordination topologies about Cu(I). The weak-field electronic characteristics and the less flexible nature of L^{Me} ligand may help create transition metal fragments that exhibit distinct reactivity. Studies addressing the reactivity of the Cu(I) and Fe(II) complexes supported by the L^{Me} ligand are currently underway in our laboratory.

Experimental Section

All reactions were performed using standard Schlenk techniques or in an MBraun Labmaster 130 drybox under an atmosphere of N_2, unless otherwise stated. All reagents were obtained from commercial vendors and were used without further purification unless otherwise noted. Anhydrous solvents were purchased from Sigma-Aldrich and further purified by sparging with Ar gas and passage over activated alumina columns. Elemental analyses were performed by Columbia Analytical Services, Tucson, AZ, or Atlantic Microlab, Inc., Norcross, GA. ^1H and ^{13}C NMR spectra were recorded on a Varian Mercury 300 MHz spectrophotometer at ambient temperature. Chemical shifts (δ) are reported in parts per million (ppm) and coupling constants (J) are reported in hertz (Hz). NMR spectra were referenced internally to residual solvent. IR spectra were recorded as KBr pellets on a Varian Scimitar 800 Series FT-IR spectrophotometer. Nujol and solution state IR spectra were recorded using the same spectrophotometer with KBr salt plates. UV−visible absorption spectra were recorded on a Cary 50 spectrophotometer using 1.0 cm quartz cuvettes. Solution-state magnetic moments were measured using the Evans' method.[63,64] Mass spectra were recorded in the Mass Spectrometry Center at Emory University on a JEOL JMS-SX102/SX102/A/E mass spectrometer. X-ray crystallography studies were carried out in the X-ray Crystallography Laboratory at Emory University on a Bruker Smart 1000 CCD diffractometer. The ligands tris(2-aminophenyl)amine, $N(o\text{-}PhNH_2)$,[39,46] and tris(2-dimethylaminoethyl)amine (Me_6tren)[16] and $[Cu(Me_6tren)]PF_6$[10] were synthesized using published literature procedures.

Tris(2-dimethylaminophenyl)amine, (L^{Me}). An aqueous formaldehyde solution (37% by weight) (6.61 mL, 88.0 mmol) was added to an acetonitrile (100 mL) solution of $N(o\text{-}PhNH_2)_3$ (0.7993 g, 2.75 mmol) and stirred. After 30 min, $NaBH_3CN$ (1.6510 g, 26.3 mmol) was added to the solution as a solid. Once all of the $NaBH_3CN$ was dissolved, concentrated HOAc (0.6 mL) was added dropwise to adjust the pH to ~7, and the reaction mixture was stirred for 12 h. All volatiles were then removed under reduced pressure to yield a sticky, off-white solid. A KOH solution (2 M, 50 mL) was added to the crude solid, and Et_2O (3×20 mL) was used to extract the product. The organic layers were combined and washed with KOH solution (0.5 M, 50 mL). The organic layer was then extracted with an aqueous HCl solution (1 M, 3×15 mL). The aqueous extracts were combined and neutralized using solid KOH. The product was then extracted using Et_2O (3×20 mL). The Et_2O washes were combined and dried over K_2CO_3. The K_2CO_3 was removed by filtration, and the filtrate concentrated to dryness using a rotary evaporator to yield a light pink solid. The light pink solid was recrystallized from hot methanol to yield the product as off-white needles (77%, 0.7959 g). 1H NMR ($CDCl_3$): 7.05 (dd, 3H, $J=1.8$, $J=7.5$), 6.98 (td, 3H, $J=1.8$, $J=6.9$), 6.86 (td, 3H, $J=1.8$, $J=7.8$), 6.78 (dd, 3H, $J=1.8$, $J=7.8$), 2.39 (s, 18H). HRMS (ESI): $C_{24}H_{30}N_4$ m/z Calcd. 375.24705 Found 375.25461 $[M+1]^+$. FTIR (KBr) $\tilde{\nu}_{max}$ (cm^{-1}): 3054, 2971, 291, 2820, 2774, 1922, 1889, 1804, 1781, 1586, 1491, 1448, 1314, 1258, 954, 753.

Preparation of $[HL^{Me}]PF_6$. Off-white crystalline L^{Me} (0.0749 g, 0.200 mmol) was dissolved in 10.0 mL of CH_3CN at room temperature. An aqueous solution of HPF_6 (~65 wt % in water, 0.0253 mL, 0.1860 mmol) was added dropwise to this solution. The reaction was stirred for 1 h. All solvent was removed from the reaction mixture using a rotary evaporator to yield a white powder. The white powder was isolated on a medium porosity frit and washed with Et_2O (3×10 mL) (0.0937 g, 0.1800 mmol, 97%). X-ray quality crystals were grown by diffusing Et_2O into a THF solution of the product. ^1H NMR 7.94 (br), 7.72 (br), 7.60 (t), 7.02 (br), 3.48 (br, N-*H*), 2.54 (br, NH−C*H*$_3$), 2.42(br, N−C*H*$_3$). FTIR (KBr) $\tilde{\nu}_{max}$ (cm^{-1}): 3139; 2991, 2851, 2741, 2685, 2538, 2427 1490, 1448, 842.95; HR-MS(ESI): $[HL^{Me}]^+$ m/z Calcd. 375.25478. Found 375.25461.

Preparation of $[Fe(Me_6tren)Cl]BPh_4$. To a slurry of $FeCl_2$ (0.0715 g, 0.5641 mmol) in CH_2Cl_2 (10.0 mL) was added a solution of Me_6tren (0.1298 g, 0.5634 mmol) in 10.0 mL of CH_2Cl_2. After stirring 30 min, $NaBPh_4$ (0.1936 g, 0.5658 mmol) was added dropwise as a MeOH solution (2 mL), and the reaction stirred for an additional 3 h. During this time a large amount of white precipitate had formed. The precipitate was isolated on a medium porosity frit and washed with CH_2Cl_2 (2×2 mL). The filtrate and CH_2Cl_2 washings were combined and concentrated to dryness to afford a white solid. Single crystals suitable for X-ray diffraction studies can be obtained by slow diffusion of Et_2O into DMF solution of the complex. FTIR (KBr) $\tilde{\nu}_{max}$ (cm^{-1}): 1950, 1886, 1825, 1764; 1579; $\nu(NMe_2)$ 1475, 1427, 736, 707. HRMS (ESI): $[Fe(Me_6tren)Cl]^+$ m/z Calcd. 321.15084. Found 321.15049 (100.00). Anal. Calcd (Found) for $[Fe(Me_6tren)Cl]BPh_4 \cdot CH_3CN$: C, 66.92 (66.91); H, 7.83 (7.96); N, 10.27 (9.87).

Preparation of $[Fe(L^{Me})Cl]BPh_4$. To a suspension of $FeCl_2$ (0.0390 g, 0.3077 mmol) in 10.0 mL of CH_2Cl_2 was added a solution of L^{Me} (0.1194 g, 0.3205 mmol) in 10.0 mL of CH_2Cl_2 dropwise. A solution of $NaBPh_4$ (0.1084 g, 0.3168 mmol) in MeOH (5 mL) was added dropwise to the reaction mixture, and a precipitate formed immediately. The reaction mixture was stirred for 4 h, and the white precipitate was removed by filtering the reaction mixture through a medium porosity frit. The filtrate was then layered with Et_2O at room temperature. Colorless needle-shaped crystals formed overnight. Colorless block crystals, suitable for X-ray diffraction, were grown by diffusing Et_2O into a concentrated acetonitrile solution of the product. UV−vis (CH_3CN) λ_{max}, nm (ε, M^{-1} cm^{-1}): 297 (sh) 610 nm (123). FTIR (KBr) $\tilde{\nu}_{max}$ (cm^{-1}): 3052, 2984, 2832, 2789, 1943, 1884, 1813, 1752; 1579, 1489, 1447, 1296, 1265, 1243, 734, 705. ^1H NMR (CD_3CN): 16.60 (br), 13.60 (br), 13.53 (br), 10.67 (br), 7.23(s), 6.97(t), 6.82(s). HRMS (ESI): $[Fe(L^{Me})Cl]^+$ m/z Calcd. 465.15084. Found 465.15053. Anal. Calcd (Found) for $[Fe(L^{Me})Cl]BPh_4$: C, 73.44 (73.31); H, 6.42 (6.63); N, 7.14 (7.05). $\mu_{eff} = 5.03$ μB (Evans Method, CD_3CN, 298 K).

Preparation of $[Co(L^{Me})Br]BPh_4$. To a stirred solution of L^{Me} (0.1862 g, 0.5 mmol) in 10.0 mL of CH_2Cl_2 was added $CoBr_2$ (0.1088 g, 0.5 mmol). The reaction was stirred for 30 min, and then $NaBPh_4$ (0.1734 g, 0.5 mmol) was added dropwise as a MeOH solution (2 mL). The reaction was refluxed under an atmosphere of N_2 for 3 h. The reaction mixture was cooled to room temperature. All volatiles were removed under reduced pressure to yield a purple precipitate. The precipitate was isolated on a medium porosity frit, washed with MeOH (10 mL), and dried under vacuum overnight (0.250 g, 60%,). Single crystals for X-ray crystallographic studies were formed by the slow diffusion of Et_2O into a concentrated CH_3CN solution of the product. Bulk recrystallization can also be used to isolate large quantities of analytical pure material by diffusion of Et_2O into THF solution of the product. ^1H NMR (CD_3CN): 19.45 (br), 14.95 (br), 14.50 (br), 8.80 (br), 7.24 (s), 6.98 (t), 6.80 (t).

(63) Evans, D. F. *J. Chem. Soc.* **1959**, 2003–2005.
(64) Sur, S. K. *J. Magn. Reson.* **1989**, *82*, 169–173.

Table 5. Crystal Data and Refinement Data

	H[L^{Me}]	[Fe(L^{Me})Cl]BPh_4	[Co(L^{Me})Br]BPh_4	[Ni(L^{Me})Cl]BPh_4	[Cu(L^{Me})Cl]BF_4	[Cu(L^{Me})CO]PF_6	[Fe(Me_6tren)Cl]BPh_4
empirical formula	$C_{24}H_{31}F_6N_4P$	$C_{48}H_{50}BClFeN_4$	$C_{50}H_{53}BBrCoN_5$	$C_{50}H_{53}BClN_5Ni$	$C_{24}H_{30}BClCuF_4N_4$	$C_{25}H_{30}CuF_6N_4OP$	$C_{38}H_{53}BClFeN_5$
crystal system	monoclinic	monoclinic	monoclinic	monoclinic	orthorhombic	monoclinic	monoclinic
space group	*P*2(1)/*c*	*Pc*	*P*2(1)/*n*	*P*2(1)/*n*	*Pna*2(1)	*P*2(1)/*n*	*Pc*
a, Å	7.792(5)	10.066(11)	12.5584(3)	12.5069(17)	9.0188(5)	11.412(6)	12.487(5)
b, Å	20.721(12)	11.957(13)	18.1423(5)	18.029(2)	21.9007(14)	14.348(7)	12.478(5)
c, Å	17.766(10)	17.111(18)	19.2187(5)	19.301(3)	12.4198(7)	16.781(8)	23.570(10)
α, deg	90	90	90	90	90	90.00	90
β, deg	101.240(10)	99.318(18)	96.238(1)	96.055(2)	90	95.398(8)	90.510(7)
γ, deg	90	90	90	90	90	90.00	90
V (Å^3)	2813(3)	2032(4)	4352.8(2)	4327.8(10)	2453.1(2)	2736(2)	3672(3)
Z	4	2	4	4	4	4	4
crystal size, mm	0.51 × 0.05 × 0.04	0.15 × 0.04 × 0.04	0.43 × 0.30 × 0.20	0.15 × 0.06 × 0.05	0.52 × 0.30 × 0.28	0.18 × 0.13 × 0.04	0.20 × 0.15 × 0.10
T, K	172(2)	173(2)	173(2)	173(2)	173(2)	173(2)	173(2)
ref. coll.	50056	34680	34427	60714	28619	57440	63558
Indep. ref. (R_{int})	7873[0.0870]	11425[0.1489]	8558[0.0611]	9157[0.2141]	8482[0.0525]	9522[0.0884]	20690[0.0623]
GOF on F^2	1.013	1.002	1.006	1.019	1.044	1.036	1.044
Final *R* indices [$I > 2\sigma(I)$]	R1 = 0.0576	R1 = 0.0592	R1 = 0.0384	R1 = 0.0670	R1 = 0.0588	R1 = 0.0551	R1 = 0.0744
	wR2 = 0.1153	wR2 = 0.0791	wR2 = 0.0871	wR2 = 0.1137	wR2 = 0.1478	wR2 = 0.1321	wR2 = 0.2028
R indices (all data)	R1 = 0.1211	R1 = 0.1963	R1 = 0.0549	R1 = 0.1734	R1 = 0.0659	R1 = 0.1075	R1 = 0.0937
	wR2 = 0.1311	wR2 = 0.1110	wR2 = 0.0950	wR2 = 0.1443	wR2 = 0.1552	wR2 = 0.1566	wR2 = 0.2151

FTIR (KBr) $\tilde{\nu}_{max}$ (cm^{-1}): 3056, 3044, 2984, 1492, 1449, 1258, 1204, 1146, 1095, 1004, 921, 773, 731, 706, 611. UV−vis (CH_3OH) λ_{max}, nm (ε, M^{-1} cm^{-1}): 510 (73), 534 (72) 620 (128). μ_{eff} = 4.68 μ_B (Evans Method, CD_3CN, 298 K). Anal. Calcd (found) for [Co(L^{Me})Br]BPh_4: C, 69.24 (68.99); H, 6.05 (6.13); N, 6.73 (6.75).

Preparation of [Ni(L^{Me})Cl]BPh_4. This complex was prepared in a manner analogous to that of [Co(L^{Me})Br]BPh_4, except $Ni(PPh_3)_2Cl_2$ was used in place of $CoBr_2$. The product was isolated as a green powder (90%, 0.3560 g). [Ni(L^{Me})Cl]BPh_4 was recrystallized for X-ray diffraction studies by the diffusion of Et_2O into a concentrated acetonitrile solution of the product. Bulk recrystallization of the crude material was achieved by diffusing Et_2O into a concentrated THF solution of the product to yield pale yellow-green needles. ^{1}H NMR (CD_3CN): 23.54 (br), 16.48 (br), 14.80 (br), 7.22, 6.97 (t), 6.82 (t), 2.21 (br). FTIR (KBr) $\tilde{\nu}_{max}$ (cm^{-1}): 3054, 3031, 2983, 2928 1492, 1426, 1426, 1259, 1198, 1144, 1094, 1032, 1005, 772, 733, 705, 613 585, 669. UV−vis (CH_3OH) λ_{max}, nm (ε, M^{-1} cm^{-1}): 440 (112), 684 (30). μ_{eff} = 3.47 μ_B (Evans Method, CD_3CN, 298 K). Anal. Calcd (found) for [Ni(L^{Me})Cl]BPh_4·THF: C, 72.62 (72.54); H, 6.80 (6.78); N, 6.51 (6.61).

Preparation of [Cu(L^{Me})Cl]BF_4. A green methanol solution (8 mL) of $CuCl_2$ (0.1338 g, 0.9952 mmol) was added to a stirring methanol solution (15 mL) of L^{Me} (0.3728 g, 0.9954 mmol) resulting in the immediate formation of a dark red reaction mixture. The reaction was stirred at room temperature for 10 min. Colorless $AgBF_4$ (0.1942 g, 0.9976 mmol) was then added dropwise as a CH_3OH solution (5 mL) to reaction mixture. The reaction mixture turned brown at once with concomitant formation of a white precipitate. The mixture was stirred overnight and filtered through a pad of Celite to remove AgCl. The filtrate was concentrated using a rotary evaporator to yield a bright yellow solid. This solid was collected on a medium porosity frit and washed with a 10:1 Et_2O/CH_3CN solution (10 mL) to yield a yellow-green solid (0.49 g, 88%). Single crystals for X-ray crystallography were grown by diffusing Et_2O into saturated CH_3CN solution of crude product. ^{1}H NMR (CD_3CN): 18.20 (br), 13.55 (br), 12.00 (br), −4.4 (br). FTIR (KBr) $\tilde{\nu}_{max}$ (cm^{-1}): 3054, 3031, 2931, 2852, 2820, 2775, 1492, 1472, 1288, 1062, 1007, 922, 732, 587, 480. UV−vis (CH_3CN) λ_{max}, nm (ε, M^{-1}cm^{-1}): 430 (sh) (1052), 782 (146), 1033 (306). Anal. Calcd (Found) for [Cu(L^{Me})Cl]BF_4: C, 51.44 (51.73); H, 5.40 (5.44); N, 10.00 (10.18). HRMS (ESI): [Cu(L^{Me})Cl]$^+$ *m*/*z* Calcd. 475.14550. Found 472.14520 (100.00). μ_{eff} = 1.83 μ_B (Evans Method, $CDCl_3$, 298 K).

Preparation of [Cu(L^{Me})]PF_6. To an CH_3CN solution (3.0 mL) of $[Cu(CH_3CN)_4]PF_6$ (0.0754 g, 0.2023 mmol) was added a solution of L^{Me} (0.0786 g, 0.2099 mmol) in CH_3CN (3 mL). The reaction was stirred at room temperature overnight. The solvent was removed under reduced pressure to afford a white power. The powder was washed with Et_2O and dried on a sintered glass frit (0.1058 g, 0.1815 mmol, 89.7%). The complex was recrystallized by layering Et_2O onto a concentrated CH_3CN solution of the product. Unfortunately, X-ray quality crystals of this complex could not be isolated. ^{1}H NMR (CD_3CN): 7.10 (3H), 7.00 (3H), 6.88 (3H), 6.70 (3H), 2.37 (18H). FTIR (KBr) $\tilde{\nu}_{max}$ (cm^{-1}): 3059, 2932, 2821, 2775, 1492, 1448, 1261, 1225, 1099, 1048, 841,771, 558. MS (EM-ESI): [Cu(L^{Me})]$^+$ *m*/*z* Calcd. 437.17665. Found 437.17560 (^{63}Cu, 100), 439.17413 (^{65}Cu, 44.33).

Preparation of [Cu(L^{Me})(CO)]PF_6. Solid [Cu(L^{Me})]PF_6 (0.0512 g, 0.0878 mmol) was dissolved in dry acetone (10 mL) and transferred to a Schlenk flask. The colorless solution was then sparged with CO gas for 30 min. Over this time period, the reaction mixture changed from colorless to light green. The resulting solution was layered with Et_2O and allowed to stand overnight, whereupon green crystals of the product formed (0.0266 g, 49.5%). Crystals suitable for X-ray crystallography were grown by diffusing Et_2O into a THF solution of the complex. ^{1}H NMR (CD_3CN): 7.16 (3H), 7.00(3H), 6.85 (3H), 6.66 (3H) 2.37 (18H). FTIR (KBr) $\tilde{\nu}_{max}$ (cm^{-1}): 3072, 2884, 2813, (CO) 2088, 1493, 1449, 1271, 1218, 1101, 1051, 1019, 840, 768, 558. FTIR (THF) $\tilde{\nu}_{max}$ (cm^{-1}): (CO) 2094. FTIR (Nujol) $\tilde{\nu}_{max}$ (cm^{-1}): (CO) 2088.

Preparation of [Cu(Me_6tren)(CO)]PF_6. Under an inert atmosphere, a Schlenk flask was charged with Me_6tren (0.10 g, 0.44 mmol), 10.0 mL of THF, and a stir bar and sealed with a septum. In a separate Schlenk flask, $[Cu(CH_3CN)_4]PF_6$ (0.16 g, 0.44 mmol) was dissolved in THF and fitted with a septum. Both solutions were then saturated with CO (g) by bubbling each solution with $CO_{(g)}$ for 30 min. The $[Cu(CH_3CN)_4]PF_6$ solution was transferred to the Me_6tren solution via cannula. The reaction mixture changed from colorless to pale green immediately. The reaction mixture was layered with Et_2O and allowed to stand overnight, producing a pale green microcrystalline powder. The solid was collected on a frit and washed with Et_2O (0.150 g, 88%). The pale green solid is very reactive toward O_2 and difficult to store as a solid or in solution for long periods of time.

FTIR (THF) $\tilde{\nu}_{max}$ (cm^{-1}) (CO) 2078; FTIR (CH_3CN) $\tilde{\nu}_{max}$ (cm^{-1}): (CO) 2085; FTIR (Nujol) $\tilde{\nu}_{max}$ (cm^{-1}) (CO) 2098.

Infrared Spectroscopies of Carbonyl Complexes. The solution-state IR spectra for $[Cu(L^{Me})(CO)]PF_6$ and $[Cu(Me_6tren)(CO)]PF_6$ were recorded by a modified literature procedure.[12] In a 20.0 mL scintillation vial, solid complex (~10−12 mg) was dissolved in in 2.0 mL of solvent. The vial was fitted with a septum, removed from the drybox and sparged with anhydrous $CO_{(g)}$ for one minute. A gastight syringe was used to transfer the solution to a solution IR cell (Internation Crystal Laboratories, 0.10 mm path length) fitted with two septa under a constant stream of $CO_{(g)}$.

X-ray Diffraction Studies. Suitable crystals of $[HL^{Me}]PF_6$, $[Fe(Me_6tren)Cl]BPh_4$, $[Fe(L^{Me})Cl]BPh_4$, $[Co(L^{Me})Br]BPh_4$, $[Ni(L^{Me})Cl]BPh_4$, $[Cu(L^{Me})Cl]BF_4$, and $[Cu(L^{Me})CO]PF_6$ were coated with Paratone N oil, suspended in a small fiber loop, and placed in a cooled nitrogen gas stream at 173 K on a Bruker D8 APEX II CCD sealed tube diffractometer with graphite monochromated MoKα (0.71073 Å) radiation. Data were measured using a series of combinations of φ and ω scans with 10 s frame exposures and 0.5° frame widths. Data collection, indexing, and initial cell refinements were all carried out using APEX II[65] software. Frame integration and final cell refinements were done using the SAINT[66] software. All structures were solved using Direct methods and difference Fourier techniques (SHELXTL, V6.12).[67] Hydrogen atoms were placed in their expected chemical positions using the HFIX command and were included in the final cycles of least-squares with isotropic *U*ij's related to the atom's ridden upon. All non-hydrogen atoms were refined anisotropically except for the acetonitrile solvent molecules in $[Fe(Me_6tren)Cl]BPh_4$, $[Co(L^{Me})Br]BPh_4$, and $[Ni(L^{Me})Cl]BPh_4$ and the disordered F atoms in $[Cu(L^{Me})(CO)]PF_6$. Scattering factors and anomalous dispersion corrections are taken from the International Tables for X-ray Crystallography.[68] Structure solution, refinement, graphics, and generation of publication materials were performed by using SHELXTL, V6.12 software. Additional details of data collection and structure refinement are given in Table 5. CCDC 766572−766578 contain the supplementary crystallographic data for this manuscript. These files can be obtained free of charge from the Cambridge Crystallographic Data Centre via http://www.ccdc.cam.ac.uk/data_request.cif.

Acknowledgment. We thank Dr. Rui Cao and Ms. Sheri Lense for crystallographic assistance. The University Research Committee of Emory University is acknowledged for financial support.

Supporting Information Available: Crystallographic data in CIF format. This material is available free of charge via the Internet at http://pubs.acs.org.

(65) *APEX II, 2005*; Bruker AXS, Inc.: Madison, WI, 2005.
(66) *SAINT*, Version 6.45A; Bruker AXS, Inc.: Madison, WI, 2003.
(67) Sheldrick, G. M. *Acta Crystallogr., Sect. A: Found. Crystallogr.* **2008**, *A64*(1), 112–122.
(68) Wilson, A. J. C., Ed.; *International Tables for X-ray Crystallography, Vol. C.*; Kynoch, Academic Publishers: Dordrecht, The Netherlands, 1992.